



HAL
open science

Genome-wide screen for genes with effects on distinct iron uptake activities in *Saccharomyces cerevisiae*

Emmanuel Lesuisse, Simon A.B. Knight, Maïte Courel, Renata Santos, Jean-Michel Camadro, Andrew Dancis

► To cite this version:

Emmanuel Lesuisse, Simon A.B. Knight, Maïte Courel, Renata Santos, Jean-Michel Camadro, et al.. Genome-wide screen for genes with effects on distinct iron uptake activities in *Saccharomyces cerevisiae*. *Genetics*, 2005, 169 (1), pp.107-122. 10.1534/genetics.104.035873 . hal-00007533

HAL Id: hal-00007533

<https://hal.science/hal-00007533>

Submitted on 25 Oct 2005

HAL is a multi-disciplinary open access archive for the deposit and dissemination of scientific research documents, whether they are published or not. The documents may come from teaching and research institutions in France or abroad, or from public or private research centers.

L'archive ouverte pluridisciplinaire **HAL**, est destinée au dépôt et à la diffusion de documents scientifiques de niveau recherche, publiés ou non, émanant des établissements d'enseignement et de recherche français ou étrangers, des laboratoires publics ou privés.

Genome-wide screen for genes with effects on distinct iron uptake activities in *Saccharomyces cerevisiae*

Emmanuel Lesuisse*, Simon A. B. Knight†, Maïté Courel*, Renata Santos*, Jean-Michel Camadro* and Andrew Dancis†

* Laboratoire d'Ingénierie des Protéines et Contrôle Métabolique, Département de Biologie des Génomes, Institut Jacques Monod, Unité Mixte de Recherche 7592 CNRS-Universités Paris 6 and 7, France.

† Department of Medicine, Division of Hematology-Oncology, University of Pennsylvania, Philadelphia, PA 19104;

Corresponding author: Emmanuel Lesuisse, Laboratoire d'Ingénierie des Protéines et Contrôle Métabolique, Institut Jacques Monod, Tour 43, Université Paris 6 and Paris 7, 2 place Jussieu, F-75251 Paris cedex 05, France. E-mail: lesuisse@ijm.jussieu.fr

Tel : (33) 1 44 27 63 56

Fax : (33) 1 44 27 57 16

SUMMARY

We screened a collection of 4847 haploid knockout strains (EUROSCARF collection) of *Saccharomyces cerevisiae* for iron uptake from the siderophore ferrioxamine B (FOB). A large number of mutants showed altered uptake activities, and a few turned yellow when grown on agar plates with added FOB, indicating increased intracellular accumulation of undissociated siderophore. A subset consisting of 197 knockouts with altered uptake were examined further for regulated activities that mediate cellular uptake of iron from other siderophores or from iron salts. Hierarchical clustering analysis grouped the data according to iron sources and according to mutant categories. In the first analysis, siderophores grouped together with the exception of enterobactin, which grouped with iron salts, suggesting a reductive pathway of iron uptake for this siderophore. Mutant groupings included three categories: i) high FOB uptake, high reductase, low ferrous transport; ii) isolated high or low FOB transport; and iii) induction of all activities. Mutants with statistically altered uptake activities included genes encoding proteins with predominant localization in the secretory pathway, nucleus and mitochondria. Measurements of different iron uptake activities in the yeast knockout collection makes possible distinctions between genes with general effects on iron metabolism and those with pathway specific effects.

Keywords: iron, genome, yeast, siderophore.

Abbreviations: FOB, ferrioxamine B; FCH, ferrichrome; CG, coprogen; ENB, enterobactin; TAF, triacetylfulvarinine C; FC, ferricrocin; BPS, bathophenanthroline disulfonic acid; ORF, open reading frame.

INTRODUCTION

Recent advances have made possible genome wide approaches to the biology of eukaryotes. Many genes and proteins implicated in iron metabolism have been identified in the past ten years using classical genetic approaches of mutagenesis, phenotype screening, complementation and homology searching. More recently global transcriptome analysis has become possible, and the effects of iron manipulations on gene expression have been studied. Using these methods a number of iron

transporters and regulators have been discovered (KOSMAN 2003). However, many things are still missing from a complete picture of cellular iron metabolism. There must exist mediators of intracellular iron trafficking, distribution, organelle transport, and processing – few of which are yet identified. Regulators coordinating use of iron in cofactors such as heme and Fe-S must exist and the cofactors must be made, trafficked and delivered to target apoproteins. Most of these key components are yet to be found. Finally, essential processes such as

transcription, translation, protein trafficking, organelle biogenesis and secretion are likely to influence iron metabolism to different degrees and in different manners. A new tool, the haploid knockout collection of *S. cerevisiae*, has recently become available. Each strain carries a complete deletion of a single ORF, and the collection can be manipulated and examined in microtiter well format. We wondered whether we could use this collection to discover novel genes involved in iron metabolism.

The idea underlying this screen is that yeast expresses two independent pathways by which iron can enter cells – siderophore and reductive (DANCIS et al. 1990; LESUISSE and LABBE 1989). Both pathways are regulated and responsive to iron availability (YUN et al. 2000a). Therefore, random or targeted mutations in the genome that alter basic processes involved in cellular iron metabolism will affect activities for both pathways. By contrast, mutations selectively impacting one or the other system will be due to altered expression, localization or function of pathway specific components.

The siderophore pathway mediates iron uptake from siderophores (LESUISSE et al. 2001; YUN et al. 2000b). These are small molecules that bind, solubilize and chelate ferric iron in the environment with tremendous affinity. They are synthesized by a non-ribosomal enzymatic process and secreted by bacteria and fungi, although not by *S. cerevisiae*. This yeast, however, has evolved means for acquiring iron from siderophores made by other organisms. Plasma membrane transporters belonging to the multifacilitator superfamily are required for internalization of ferrisiderophore complexes (HEYMANN et al. 1999; LESUISSE et al. 1998; YUN et al. 2000b). Trafficking into a vesicular compartment and release of iron occurs subsequently (KIM et al. 2002). Intracellular release of iron from siderophores is probably mediated by special reductases and/or hydrolases. The details of intracellular trafficking of ferrisiderophores, iron release from ferrisiderophores and iron distribution following release are still undefined (reviewed by Haas (HAAS 2003)).

The reductive pathway mediates iron uptake from ferric chelates (reviewed by Kosman (KOSMAN 2003)). An externally directed plasma membrane ferric reductase activity dependent on Fre1 (DANCIS et al. 1992) and Fre2 (GEORGATSOU and ALEXANDRAKI 1994) is able to reduce ferric chelates of varying composition (including siderophores), thereby releasing ferrous iron that can be accessed by the high-affinity ferrous transport complex. The latter consists of two components, a multi-copper oxidase (Fet3) with externally directed oxidase domain and a polytopic permease protein (Ftr1) (STEARMAN et al. 1996). The two components together mediate high-

affinity transport of iron into the cell, and both are required for this activity. Copper plays a special role in the reductive pathway, because copper is an obligate cofactor for the multi-copper oxidase (DANCIS et al. 1994). Copper delivery to the oxidase requires cellular copper uptake (mediated by Ctr1 and in some strains also by Ctr3) and copper delivery into the secretory pathway (mediated by the Atx1 metallochaperone and the Ccc2 P-type ATPase). Thus mutations that interfere with these steps or with the integrity of the secretory pathway result in defects of reductive iron uptake. Of note, copper proteins are not involved in iron uptake from siderophores (KNIGHT et al. 2002; KOSMAN 2003).

Both siderophore and reductive pathways for iron uptake are regulated in response to iron availability. Induction occurs under conditions of low iron and is mediated by binding of the Aft1 or Aft2 proteins to consensus sequence sites in the promoters of target genes (BLAISEAU et al. 2001; RUTHERFORD et al. 2001; YAMAGUCHI-IWAI et al. 1996). Expression of genes for both reductive and siderophore iron uptake are under control of Aft1/2, although their regulatory controls are not perfectly coordinated; modifying effects of other factors are likely to occur on the individual promoters. For example, siderophore uptake seems to turn on in response to more severe iron deprivation, and reductive iron uptake responds to milder iron deprivation. A class of mutants with defects in Fe-S cluster assembly exhibits a complex iron regulatory phenotype characterized by global effects on basic aspects of iron metabolism. Impaired iron-sulfur cluster assembly leads to constitutive Aft1/2 dependent gene expression and pleiomorphic phenotypes including activation of both reductive and siderophore uptake systems. Within the cells of these mutants, iron accumulates within mitochondria and iron-sulfur cluster protein activities are deficient. (JENSEN et al. 2004).

Here we screened a collection of 4847 haploid knockout strains (collection from EUROSCARF) of *S. cerevisiae* for regulated activities that mediate cellular uptake of iron from siderophores or from ferric/ferrous salts. We identified hundreds of genes with effects on one or more of these activities. A subset of these was evaluated as homozygous diploid knockouts to decrease problems with suppressor mutations. Some of these genes were previously known to be involved in iron handling, although most were not previously connected to iron metabolism. An advantage of the present strategy is that it did not depend on evaluation of growth, which can be difficult to score and insensitive to subtle changes in iron homeostasis.

MATERIALS AND METHODS

Yeast strains and growth conditions: The entire collection of haploid knockout strains and a subset of diploid knockout strains of *S. cerevisiae* (constructed in BY4741 and BY4743, respectively) were purchased from the European *Saccharomyces cerevisiae* Archive for Functional Analysis (EUROSCARF, Frankfurt, Germany). Genotype of the wild type strains is: *MATa*; *his3Δ1*; *leu2Δ0*; *met15Δ0*; *ura3Δ0* (BY4741); *MATa/MATα*; *his3Δ1/his3Δ1*; *leu2Δ0/leu2Δ0*; *met15Δ0/MET15*; *LYS2/lys2Δ0*; *ura3Δ0/ura3Δ0* (BY4743). The cells were grown in the wells of microtiter plates filled with complete YPD medium (100 μ l medium /well). The cells were precultured for 48 h at 30°C without agitation and then diluted 10-fold in medium of the same composition and cultured for 5 h under the same conditions before being used for experiments. For quality control, one mutant strain was randomly selected from each of 6 plates (YLR363w, YNR031c, YML033w, YLR278c, YOR041c, YOR356w) and subjected to two PCR reactions for strain verification. The primers used were strain specific primers A and KanB to detect the deleted gene, and A and B to detect the wild-type gene. Primers were listed on the web site for the Saccharomyces Genome Deletion Project. In each case, the correct deleted gene was detected and the wild-type allele was not detected, indicating that the well contained the correct strain deletion and furthermore that there was no evidence of contamination with other yeast strains.

Screens for siderophore uptake: The ^{55}Fe -labeled siderophore (FOB, FCH, TAF or ENB) was added to the wells of the culture plates at a final concentration of 1 μM , and the cells were grown for 2 h at 30°C. The cells were then collected with a cell harvester (Brandel) and washed with water on the filter (Wallac) before scintillation counting (Wallac Trilux MicroBeta).

Ferric reductase and ferrous uptake assays: Cells were inoculated and grown as described above. After the 5 h growth at 30°C, the microtiter plates were centrifuged 1500 x g for 5min. The medium was aspirated, and the cells were washed twice in ice cold 50 mM citrate pH 6.6, 5 % D-glucose and resuspended in 100 μ l of the same. Optical density of the cell suspension was measured. For measurement of ferric reductase activity, 80 μ l of the cell suspension was aliquoted to a fresh 96-well plate, and the assay solution of citrate buffer containing final concentrations of 1 mM ferric ammonium sulfate and 1 mM bathophenanthrolinedisulfonate (BPS) was added. After 2 h incubation, absorbance of the ferrous-BPS complex was measured at 515 nm. The remaining cells were resuspended in 1 μM ^{55}Fe citrate

and incubated at 30°C. After 1h, the cells were harvested (Tomtec Mach III M) onto fiber filters (Wallac). The filters were allowed to dry, and they were then soaked in scintillation fluid (Wallac BetaPlate Scint) before being counted using a 96-well liquid scintillation counter (Wallac Microbeta LS).

Clustering of data: Mutant strains with similar patterns of activities for iron reductase, ferrous iron uptake and siderophore iron uptake were identified by clustering analysis of the numerical data. Activities in the mutant strains were normalized by reference to the wild-type values, and these ratios were expressed as log base 2. We used the Cluster 3.0 software developed by Eisen *et al.* (EISEN *et al.* 1998) and modified by de Hoon *et al.* (DE HOON *et al.* 2004) to perform k-mean clustering (k=10) of the data, with uncentered correlation for similarity metric for both strains (row) and activities (columns). Cluster 3.0 was retrieved at <http://bonsai.ims.u-tokyo.ac.jp/~mdehoon/software/cluster>

The output was visualized using the JavaTreeView software written by A. Saldanha (available at <http://genome-www.stanford.edu/~alok/TreeView>).

Statistical Analysis: The diploid strains assayed for ferric reductase and ferrous uptake activities were assayed a total of four times. A regression analysis in the context of ANOVA was used to compare each mutant strain to the wild-type (BY4743) to test for statistical differences. The regression is equivalent to multiple paired tests of each mutant with the wild type, in turn. The underlying model for the ANOVA assumes that the population variances in each gene group are equal. A comparison of variances of the wild-type and the pooled mutants showed no significant difference in variances between the two groups. Significance level was set at p-value <0.05.

RNA analysis: For experiments requiring RNA isolation, cells were grown in complete YPD medium. After overnight pre-culture, the cells were diluted 10-fold and grown for 5 h at 30°C before RNA isolation. RNA was extracted as described previously (KOHNER and DOMDEY 1991). Northern blotting (using 20 μg of total RNA) and hybridization (at 42°C in 50% [vol/vol] formamide) were done essentially as described (SAMBROOK *et al.* 1989). The ^{32}P -labelled DNA fragments used as probes came from PCRs with the following primer sets: *FET3* (623-bp): 5'-TTCTTGGACGATTCTACTT-3' and 5'-GCAACTCTGGCAAACCTTCTA-3'; *SIT1* (872-bp): 5'-ACGCTAACCCACATCTTCTCC-3' and 5'-TAACACTACAACCCAACCAA-3'; A 1.2-kb *Bam*HI-*Hind*III fragment was used for the *ACT1* gene.

Other: The desferri-siderophores CG and ENB were purchased from EMC microcollection GmbH

(Germany). Desferri-FCH was purchased from Sigma. FOB refers to the commercially available mesylate derivative, Desferal (Novartis AG). TAF was a gift from Dr H. Haas (Department of Molecular Biology, Medical University of Innsbruck, Austria). Protoplasts were lysed and fractionated to purify isolated mitochondria as previously described (RAGUZZI et al. 1988).

RESULTS AND DISCUSSION

Initial screening of the haploid knockout collection for FOB uptake rates: The collection of haploid knockout strains was evaluated using a quantitative assay for radioactive iron uptake from FOB. Results of the screen are shown as a scattergram (Fig. 1), and they show a wide distribution of activities, with about 10% of clones exhibiting increased activity of greater than 1.8 fold wild type. The number of clones exhibiting decreased activity (less than 0.6 fold wild type) was significantly less, amounting to about 1%, but this may be due to lowered detection sensitivity for a decreased FOB uptake phenotype. The assays were repeated 3 times and a subset of strains with reproducibly abnormal uptake was selected for further study.

The FOB ferrisiderophore complex is colored yellow brown, whereas the iron free siderophore is uncolored. Yeast strains, such as *AFT1-I^{up}*, that accumulate FOB, yet are unable to dissociate the iron from the siderophore form distinctive yellow colonies (LESUISSE et al. 2001). We screened the whole collection of haploid mutants for this phenotype. Seven mutants turned yellow due to accumulation of undissociated FOB (Fig. 2). *SPT4* (YGR063c, involved in RNA elongation) and YGR064w (unknown function) are overlapping genes, and thus further study will be required to establish which of these two genes is responsible for the observed phenotype. Other strains showing the same phenotype were mutated in *CIK1* (involved in organization of microtubule arrays), *TIM18* (translocase of the inner mitochondrial membrane), *GGA2* (adaptor protein involved in Golgi to vacuole transport of special protein substrates), *GGC1* (which we previously described as *YHMI* (LESUISSE et al. 2004), a GTP/GDP exchanger of the mitochondrial inner membrane (VOZZA et al. 2004) that is involved in mitochondrial iron homeostasis). Finally, YLL029w encodes a gene with unknown function (Fig. 2). The color of colonies grown on FOB-containing agar plates was not directly related to the rate of FOB uptake by the cells, as illustrated by the *ARF1* mutant which showed high FOB uptake and no color change indicative of ferrisiderophore accumulation (Fig. 2). The colored colony phenotype therefore must reflect a specific defect in intracellular

FOB dissociation that is separate from induction of the rate of cellular FOB uptake. Little is known about the mechanisms of intracellular iron release from internalized siderophores in *S. cerevisiae*. Theoretically, iron could be released from siderophores within cells by reduction of the chelated iron or by hydrolysis of the siderophore itself. The process could take place in a vesicular compartment or in the cytoplasm and might involve regulatory effects depending on mitochondrial function. The effects on this process observed in the mutants identified here could be direct or indirect. For example, Tim18, a chaperone protein of the IMS is involved in translocation and membrane insertion of carrier proteins. Ggc1 is such a carrier protein and therefore likely to depend on Tim18 function for correct localization and folding. Guanine nucleotides in turn are the substrate for Ggc1. Levels of guanine nucleotides apparently affect iron homeostasis and might influence siderophore iron release as well, although how these effects occur is unknown. The FOB accumulator phenotype of *AFT1-I^{up}* mutants could indicate that Aft1 target genes mediate the effect, although none of the genes identified here are Aft1 regulated.

Candidate gene(s) for proteins directly participating in iron dissociation from FOB (some reductase or hydrolase, for example) were not identified here. Perhaps this is due to the nature of the screen itself. Mutant cells unable to dissociate siderophores at the intracellular level are expected to show increased siderophore uptake compared to wild-type cells when grown on siderophore-containing medium (because undissociated iron will be unavailable for Aft-mediated sensing). In the present screen, we selected strains grown on siderophore-free medium that showed high FOB uptake, thus excluding putative mutants that would show unrepressed siderophore uptake because of a defect in siderophore iron sensing. In summary, the data of Fig. 2 show that YGR063c/ YGR064w, YLL029w, *CIK1*, *TIM18*, *GGA2* and *GGC1* are involved, maybe indirectly but specifically, in iron removal from intracellular FOB.

Our screen revealed that a special category of mutants was deregulated for FOB uptake: mutants that were affected in mitochondrial functions frequently showed high (1.5-2 fold the wild-type value) or very high (more than 2 fold the wild-type value) FOB uptake rates. This was the case for mutants deleted from genes encoding mitochondrial ribosomal proteins (*MRP(L)* genes), for Δ *cox* mutants and for Δ *atp* mutants (data not shown). We are currently studying these categories of mutants further in order to discriminate between specific effects and effects related to the rho minus status of

mutants. Results of this study will be presented elsewhere.

During the course of working with the haploid mutants, we noticed that numerous strains showed changes in their uptake rates from one assay to the next. The changes were invariably from high uptake to lower uptake, and the changes became more pronounced over time and with repeated assaying (Table I). We previously found that *ssq1* and *yfh1* mutant strains developed extragenic suppressor mutations in the genes mediating cellular iron uptake (LESUISSE et al. 2003; STEARMAN et al. 1996), and iron accumulation has been shown to produce a mutator phenotype (KARTHIKEYAN et al. 2002). We therefore became concerned that extragenic suppressor mutations arising in high uptake mutant strains of the haploid knockout collection might be obscuring the true phenotypes. At this point, the haploid knockouts identified by the primary screen were re-acquired as diploids carrying deletions of the corresponding ORFs. We reasoned that these would maintain more stable phenotypes, since recessive suppressor mutations would not be expressed. We also acquired the wild type, BY4743, and seven additional homozygous diploid mutants of genes previously characterized in iron uptake and homeostasis (*FTR1*, *FET3*, *CTR1*, *ATX1*, *CCC2*, *SSQ1*, and *YHMI*) to serve as controls.

Analysis of uptake from various siderophores: A subset of the homozygous diploid mutants that showed a clear FOB uptake phenotype was analyzed for iron uptake from four different siderophores (FOB, FCH, TAF, ENB). To further parse phenotypic categories, iron and copper content of the growth medium was manipulated, and reductase and ferrous iron uptake activities were measured. This first analysis sheds light on the overlap or differences among iron uptake pathways. The data are shown in Fig. 3. Each vertical column depicts data for a particular type of iron uptake assay –ferric reductase, ferrous iron uptake, or siderophore iron uptake. Each horizontal row depicts the results for a single knockout clone, constructed by replacement of the open reading frame for a single gene, indicated by ORF number and name. The data represent mean values of triplicate measurements and are color coded, with red representing relative increased activity and green representing relative decreased activity compared to the parental control strain. The clustering software grouped the iron assays into three main nodes. The left-hand node consists in ferric reductase activity, measured following growth with low copper (-Cu), copper replete (+Cu) or low iron (BPS). These correspond to moderately inducing, repressing and maximally inducing conditions. The

middle node groups ENB uptake with ferrous uptake, following low copper (-Cu) or copper replete (-Cu) growth. The right hand node groups siderophore uptake from FOB, FCH or TAF. What is immediately clear is that although these activities involved in iron acquisition may sometimes be coordinately expressed, they more often show divergent levels of expression. The divergences are particularly informative here, and we will discuss several examples.

1) Horizontal nodes 2, 3. In these groups of mutants, ferrous uptake was low (green) and associated with increased ferric reductase activity (red). Uptake activities from siderophores FOB, FCH and TAF were increased (red). We can understand these phenotypes as consequences of a primary problem with ferrous iron transport, and a secondary regulatory response. Iron in the growth medium was present as ferric iron chelates, and so an interruption of ferrous transport will result in cellular iron depletion and generation of an iron starvation signal. Thus when uptake activities were measured, ferrous transport was low, and ferric reductase was high due to iron starvation. Similarly siderophore transport activities were induced by iron starvation experienced during growth of the cells.

2) Horizontal nodes 1 and 9. In these groups of mutants, the most striking finding is a singular increase in uptake activity for the siderophore FOB. The effect is unlikely to represent a regulatory effect from iron starvation occurring during growth, because, as stated above, FOB iron was not present in the growth media. Furthermore, other iron-regulated activities, e.g. reductase, were not induced. We are left with the conclusion that FOB uptake was specifically altered, implying a regulatory signal specific for FOB uptake or a more direct gain of function effect on components of the uptake pathway.

3) Horizontal node 5. In node 5, the FOB and FCH uptakes were increased, while other activities remained unperturbed. Again, these effects are unlikely to be the result of general misregulation of iron metabolism, because other reductase and ferrous transport were unaffected. The effects could be due to regulatory signals or upregulation of components shared by FOB and FCH uptake pathways.

4) Horizontal node 6. In two mutant strains, $\Delta sit1$ and $\Delta deg1$, iron uptake activities from FOB and FCH were decreased, whereas other activities were minimally altered. *SIT1* encodes a member of the multifacilitator family implicated in uptake of siderophores at the plasma membrane. The substrate specificity for Sit1p shows preference for FOB but also includes FCH (LESUISSE et al. 2001). The *deg1* deletion strain phenocopies $\Delta sit1$, raising the

possibility that Deg1p modulates *SITI* expression or acts downstream of Sit1p in siderophore uptake. However, the decreased FOB and FCH uptake in these knockout mutants mirrors the increased FOB and FCH uptake in other mutants (horizontal blocks 5), indicating the existence of a specific trafficking pathway for handling of these two siderophores.

5) Horizontal nodes 3, 5, 6, 10 (and to a lesser extent, 7). These groups show unique behavior for the TAF uptake activities, which remained unperturbed in the face of increased or decreased activity for transport of the other siderophores. However, in some cases TAF uptake seemed to move with the other transport activities and was clearly iron responsive. A possible explanation for these data is the existence of a threshold effect; for example, a lower affinity Aft1 binding site on a MFS member promoter mediating TAF uptake could be envisaged. Another possibility, which does not exclude the previous one, is that TAF uptake and use involves different pathways of regulation and/or trafficking. This hypothesis is strengthened by our previous observations that the presence of TAF did not interfere with the uptake of other siderophores (FCH, FOB or FC) which themselves showed complex relationships of competitive inhibition for uptake (LESUISSE et al. 2001; LESUISSE et al. 1998). In addition, we observed that the Cyc8-Tup1 repressor had opposite effects on the uptake of FOB/FCH and on the uptake of TAF (LESUISSE et al. 2001).

6) Horizontal node 8. In this node, the mutant strains showed increased cell reductase activity whatever the growth conditions and increased uptake activity whatever the iron source. This suggests that the strains grouped in this node suffer from a general misregulation of iron metabolism, as shown for mutants of mitochondrial iron homeostasis (*yfh1*, *nfs1*, *isu1/2* etc...(FOURY and TALIBI 2001; GERBER et al. 2004; LI et al. 1999)). Interestingly, 4 out of 6 strains of this node were deleted for a gene encoding a mitochondrial protein (*IMG2*, *YME1*, *MTM1* and *YHM1/GGR1*), highlighting once more the importance of the mitochondrial compartment for cellular iron homeostasis.

7) Vertical column for ENB uptake. ENB uptake was found to group with ferrous transport activities rather than with other siderophore transport activities. Siderophores bind ferric iron with high affinity but ferrous iron with low affinity. Following reduction of the ferrisiderophore complex, ferrous iron could be released and permeated into the cell *via* the Fet3/Ftr1 ferrous transport complex (LESUISSE and LABBE 1989; YUN et al. 2000a). Grouping of the ENB data with the ferrous transport data suggests that iron bound to ENB was taken up *via* a reductive pathway, and that a specific MFS member was not

involved. We sought direct confirmation for this by measuring iron uptake from various iron sources in a $\Delta fre1\Delta fre2$ mutant strain which lacks cell surface ferrireductase activity (GEORGATSOU and ALEXANDRAKI 1994). Results are shown in Fig. 4. As expected, uptake of ferric citrate was decreased in the reductase-negative mutant compared to wild-type cells (Fig. 4). This was also the case for coprogen (CG), a siderophore for which no specific receptor has been found in *S. cerevisiae* (LESUISSE et al. 1998). Uptake of hydroxamate-type siderophores for which a specific non-reductive uptake pathway has been shown unambiguously in *S. cerevisiae* (FOB, FCH, TAF), was unaffected –or even increased– by the loss of cell surface reductase activity (Fig. 4). However, uptake of the catecholate-type siderophore ENB was strongly decreased in reductase-deficient cells (Fig. 4). These results suggest that iron uptake from ENB follows a reductive pathway, and that the putative siderophore transported *via* the *ENB1* gene product remains to be identified. Another possibility is that a specific transporter for enterobactin (HEYMANN et al. 2001) could still exist and might be completely repressed in complete medium.

Analysis of gene groups with characteristic phenotypes for reductive or non-reductive uptake:

In independent experiments, a set of 110 homozygous diploid mutants, seven control strains (*FTR1*, *FET3*, *CTR1*, *ATX1*, *CCC2*, *SSQ1*, and *GGC1*) and wild-type (BY4743) were analyzed for iron uptake from FOB (siderophore pathway) and ferrous ascorbate (reductive pathway). Ferric reductase was also measured, and iron and copper content of the growth media were manipulated. The clustering analysis grouped the data to identify 10 phenotypically similar groups of mutants. These phenotypic groups could be clustered into three more general categories. The defining characteristic of the first category was low ferrous iron transport activity (Fig. 5A). The hallmark of the second category was specific alteration, (high or low) of FOB uptake activity (Fig. 5B). Finally, mutants in the third category exhibited generalized induction of all iron transport activities compared with wild-type controls (Fig. 5C). In each category, a few strains were assayed for their level of *FET3* and *SITI* RNAs by Northern blotting (Fig. 5).

1) Low ferrous uptake. The first category, characterized by low ferrous iron transport, includes knockouts of genes with known functions in iron metabolism (Fig. 5A). Within this category, the *aft1* deletion mutant exhibited a unique phenotypic profile of decreased FOB transport activity and decreased ferrous transport activity (node A-1). Basal and induced ferric reductase levels were maintained,

perhaps because of the ability of alternate transcription factors such as the copper sensing Mac1p (or Aft2p) to mediate expression in the absence of Aft1p (BLAISEAU et al. 2001; GEORGATSOU et al. 1997). *UME6* (node 5A-1) knockouts exhibited some aspects of the Δ *aft1* phenotype, and the encoded protein (a zinc finger transcription factor) may therefore play a role in iron sensing. *FET3* and *FTR1* are known Aft1p target genes. *FET3* encodes a multicopper oxidase, and the encoded protein is associated with Ftr1p to form the plasma membrane transporter complex for high-affinity ferrous uptake (STEARMAN et al. 1996). Thus, as expected, *FET3* and *FTR1* knockouts showed negligible high-affinity ferrous transport activity (node 5A-1). These mutants clustered here, although they differed from the *AFT1* deletion phenotype in that FOB uptake was not decreased in mutants of the ferrous transporter. Surprisingly, FOB uptake and ferric reductase were not induced in these iron transport mutants, implying that inactivation of the ferrous transporter does not by itself produce severe iron starvation. Other iron acquisition pathways such as low affinity iron transporters (DIX et al. 1997) likely can function in rich media to supply adequate iron to prevent starvation. This was confirmed by northern blotting *FET3* and *SIT1* mRNAs from the Δ *ftr1* mutant and from wild-type cells: transcription of these genes was only slightly increased in the mutant (Fig. 5).

Mutants blocked in riboflavin biosynthesis (Δ *rib4*, node 5A-1) also showed deregulation of iron metabolism. However, the phenotype of the haploid Δ *rib4* strain differed from that of the diploid Δ *rib4*/ Δ strain, and both the haploid and diploid strains tended to accumulate extragenic suppressor mutations (data not shown). The effect of riboflavin synthesis on iron metabolism will be described elsewhere.

Node 5A-2 clusters data for mutants of *CTR1*, *CCC2*, and *ATX1*. These mutants exhibited low ferrous transport activity, high ferric reductase and high FOB uptake. The corresponding genes have established roles in copper transport, and therefore the iron regulatory phenotypes of the mutants are likely secondary to effects on copper. *CTR1* encodes a plasma membrane copper transport protein. The function of *CTR1* is redundant with *CTR3*. However, the latter is inactivated by transposon insertion in some yeast genetic backgrounds (including BY4741/2), leading to dependence on *CTR1* expression for high-affinity copper uptake and high-affinity iron uptake (KNIGHT et al. 1996). *ATX1* encodes a copper chaperone, dedicated to delivering copper to the P-type ATPase Ccc2p, which in turn transports copper into the secretory pathway for Fet3p activation. The genes *CTR1*, *CCC2* and *ATX1* are

involved in copper handling and delivery of copper to apo-Fet3, and thus the corresponding mutants have deficient Fet3 activity accounting for the low ferrous transport activities. Another characteristic of node 5A-2 is greater induction of FOB uptake and ferric reductase compared with node 5A-1 (*FET3* and *FTR1* mutants for example). Similarly, transcription of *FET3* and *SIT1* were increased compared to wild-type levels in the Δ *ccc2*/ Δ strain representative of this node (Fig. 5). A possible explanation for these differences is provided by the role of Fet5, a multicopper oxidase associated with the Fth1 permease in the vacuole membrane and dedicated to pumping iron outward to the cytoplasm (URBANOWSKI and PIPER 1999). Thus copper deficiency or impaired copper trafficking will lead to defects in both Fet3 and Fet5 oxidases, with consequently more severe cellular iron starvation than defects in either oxidase separately. *BUD32*, *PKR1* and *RAV1* knockouts also showed similar phenotypes to the copper trafficking mutants, with low ferrous uptake partly compensated by copper addition to the media and constitutively high FOB uptake (node 5A-2). The functions of Bud32 and of Pkr1 are unclear, but Rav1 is part of a complex named 'regulator of the (H⁺)-ATPase of the vacuolar and endosomal membranes' (SEOL et al. 2001) which could be involved in copper trafficking in a way that remains to be determined.

Node 5A-3 includes protein sorting mutants localized to later stages in the secretory pathway. Also included are *VMA* mutants lacking constituents or regulators of the hydrogen transporting vacuolar ATPase. The iron phenotype of these mutants depended on transcriptional effects on iron transporter expression and also probably on post-transcriptional effects. Representative mutants of node 5A-3 (Δ *pep12* and Δ *vma6*) showed a significant increase in the levels of *FET3* and *SIT1* transcription (Fig. 5). Several mutants (Δ *pep12*, Δ *vps15*, Δ *arf1*...) with impaired endosome fusion with late endosome and vacuolar compartments are expected to exhibit decreased recycling of Sit1 (KIM et al. 2002). Increased Sit1 at the cell surface in these mutants could then enhance cellular uptake of FOB by a post-transcriptional mechanism.

The signature iron phenotype of these mutants overlaps that produced by copper deficiency, and could be explained by missorting of copper transporters and/or copper delivery components. Alternatively, disruption of acidification of the secretory pathway might interfere with efficient copper loading of apoproteins. Consistent with this idea, some ferrous transport defects in some of the mutants were corrected by growth in high concentrations of copper (50 μ M added to YPAD). The degree of correction was variable. No correction

was observed for *FET3* and *FTR1* mutants as expected, since the copper binding target Fet3p is absent or retained in the earliest part of the secretory pathway. Partial correction was observed for *CTR1*, *ATX1* and *CCC2* mutants. Some *VPS* mutants, such as *Δvps4* and *Δvps9* showed partial correction. The phenotypes of these diploid mutants in the BY4743 background were slightly different from previously published experience with haploid mutants in a different genetic (YUAN et al. 1997). However, these differences are difficult to interpret, because the ability of copper to correct ferrous transport defects in various mutants is poorly understood. The effects are presumed to be mediated by an uncharacterized low-affinity copper transport pathway able to bypass the usual copper delivery pathway to Fet oxidases in the secretory pathway.

2) Altered FOB transport. The second phenotypic category is characterized by altered FOB transport activity (Fig. 5B). Iron use from siderophores involves a complex machinery regulated at transcriptional and post-transcriptional levels. The presence of siderophores in the medium has to be «sensed» by the cells prior to the siderophore receptors being exported at the plasma membrane (KIM et al. 2002). Transcription of genes for these receptors is itself subject to complex regulation, depending on Aft1/2 and Tup1/Cyc8 (LESUISSE et al. 2001). Iron dependent and iron independent signals are integrated in control of these genes. Endocytosis and recycling of the siderophore receptors depend on the machinery for intracellular protein trafficking, involving many regulatory steps at various levels. This may explain the high number of genes implicated in FOB uptake and regulation.

In node 5B-1, FOB uptake was increased but reductase and ferrous transport were not altered. In node 5B-2, FOB uptake was increased and ferric reductase was decreased under some conditions, while ferrous transport was variable. The phenotype of these mutants was probably not due to direct transcriptional effects on the «iron regulon» genes, as the levels of *FET3* and *SITI* transcription were not significantly altered in representative strains (*Δgga2*, *Δvam6*, *Δssn8*) (Fig. 5). Many genes of these first 2 nodes (5B-1, 5B-2) are involved in transcriptional regulation and RNA processing (*LSM1*, *LSM6*, *LSM7*, *PAT1*, *SSN3*, *CYC8*, *SSN8*, *MED1*...). Thus, effects of these mutants on FOB uptake are likely to be indirect (in view of lack of change in *SITI* message level in the *Δssn8* strain). Other genes in this group are involved in intracellular protein trafficking (*GGA2*, *VAM6*, *APS3*...), and these might influence trafficking of siderophores or siderophore receptors. One of these genes, *GGA2* (block 5B-1), is particularly interesting, since the corresponding

mutant showed strongly increased FOB uptake with unaltered *SITI* transcription, while other iron-dependent activities (reductase and ferrous transport) were unchanged. Moreover, TAF uptake by the *Δgga2* mutant was unaltered (see Fig. 3, node 5), and undissociated FOB accumulated in this mutant (see Fig. 2). Thus, *gga2* mutation creates a specific interruption upstream of the dissociation step for FOB and FCH. Gga proteins are known to contribute to protein sorting by functioning as adaptors between cargo proteins and clathrin coats (KATZMANN et al. 2002). We are currently trying to use the *Δgga2* mutant as a tool to determine which cellular compartment(s) is (are) involved in iron dissociation from FOB.

The node 5B-3 is very interesting. It includes two strains mutated in genes that are anti-sense to one another, *BUD25* and *HEM14*. Both strains showed markedly increased FOB uptake, strongly decreased reductase, and unaltered ferrous transport. Both strains showed heme deficiency, although the Hem14 block in heme biosynthesis is a little leaky, because protoporphyrinogen can be oxidized into protoporphyrin non-enzymatically to some extent (CAMADRO et al. 1994). Both strains were able to grow slowly on YPD medium without supplementation with hemein or tween/ergosterol. Reductase activity of these strains was virtually absent, probably due to the lack of heme, which is a cofactor for the Fre protein reductases (SHATWELL et al. 1996). The observation that these strains showed very high uptake of FOB raises the question of the role of heme synthesis in iron homeostasis. In a recent study, Crisp *et al.* (CRISP et al. 2003) showed that heme-deficient mutants down-regulated genes of the «iron regulon». However, regulation of genes involved in siderophore uptake by these mutants was not examined. The present study shows that *SITI* transcription was tremendously increased in the *Δhem14* mutant compared to wild type cells (Fig. 5), which could account for the observed phenotype of high FOB uptake. In a previous study, we showed that some heme mutants showed constitutively high FOB uptake (LESUISSE and LABBE 1989). We therefore studied this question further, and analyzed the influence of global heme deficiency and of specific genes (*HEM* gene family and the *BUD25* gene) on siderophore and ferrous transport. Results of this study will be published elsewhere.

Node 5B-4 groups strains with low FOB uptake activities. As expected, the *Δsit1* mutant was found in this group. The influence of *HSP12* disruption on iron metabolism should be studied further, because the haploid and diploid mutants behaved differently. The haploid *Δhsp12* strain was initially selected for high FOB uptake, but tended to

lose this phenotype in the successive screens (see Table 1), while the diploid $\Delta hsp12/\Delta$ strain showed stable low FOB uptake phenotype. The reason for such a discrepancy is unknown. The phenotype of the $\Delta deg1$ strain resembles the $\Delta sit1$ strain. *DEG1* encodes a tRNA pseudouridine synthase and may play in regulating *SIT1* expression or activity. Of note, the level of *SIT1* transcript was very low in this strain (Fig. 5).

3) Generalized induction of all activities. The third phenotypic category (Fig. 5C) groups together mutants that showed highly induced reductase, FOB transport and ferrous transport. The corresponding ORFs are candidates for genes that function in general iron metabolism or iron sensing. Many categories of genes are included here, including genes for nuclear encoded mitochondrial functions, genes implicated in endocytosis, vacuolar protein sorting, and transcriptional regulators. Transcriptional and post-transcriptional effects were involved in producing the mutant phenotypes. One strain taken as representative of node 5C-1 (YLL029w) showed a moderate increase (about 2-fold) in the level of *FET3* and *SIT1* transcripts (Fig. 5). However, iron uptake activities were more severely affected (about 5-fold increased) suggesting that post-transcriptional regulation was also involved. In node 5C-2, a number of genes implicated in endocytosis and intracellular protein trafficking are grouped together. In contrast to what was observed in other endocytosis mutants (see strains of node 5A-3), no direct effect on *FET3* and/or *SIT1* transcription was observed here (Fig. 5). Note that the biological significance of low ferrous transport following growth in the presence of copper is unclear, but nonetheless, this characteristic seems to enable phenotypic grouping of endocytosis mutants. Several of the mutants in this node (*Δsnf7*, *Δvps20*, *Δvps25*, *Δvps28*, *Δvps36*, *Δbro1*) are expected to be defective in fusion of late endosome vesicles to the vacuole (KATZMANN et al. 2002). The consequences of this organellar trafficking abnormality may be to increase Sit1p concentration at the cell surface, leading to increased FOB uptake. In addition there may be enhanced surface expression of reductase and ferrous transport proteins, leading to increased reductase activity and ferrous transport activity.

Statistical analysis of mutants with effects on iron uptake grouped according to proposed cellular localizations of the corresponding gene products:

The data up to this point have been analyzed using k-means clustering of uptake and reductase activities to group mutants according to phenotypic similarities. The multiple biological replicates (n=4) of the data for ferrireductase and ferrous uptake allowed us to

perform a more standard statistical analysis (regression in the context of ANOVA) comparing each mutant with the wild type. For this analysis only diploid mutants that had a FOB uptake rate of less than or equal to 0.6X wild type (low) and of more than or equal to 1.8X wild type (high) were included. The data from this alternative statistical analysis is presented according to the proposed cellular localization of the corresponding proteins (from SGD GO annotations) in Table 2. For ferric reductase activity and ferrous uptake, mutants are described with high or low activity if there was a statistical difference compared to wild type at a level of $p < 0.05$. An overview of this table indicates the majority of mutants that had altered FOB uptake also had altered ferrireductase activity. However, of the 81 mutants that had high FOB uptake only 28 of these had significantly altered ferrous uptake (7 had high and 21 had low ferrous uptake -not including the mutant control strains). Likewise, of the five mutants that had low FOB uptake only 1 mutant also had abnormal (low) ferrous uptake. Thus comparison of FOB uptake with ferrous uptake is likely to be more informative than with ferrireductase. The lack of correlation between FOB and ferrous uptake in these mutants is probably reflective of the functional separation of these two pathways in bringing iron into the cell. However, organelles in which the FOB and ferrous uptake phenotypes converge might be key components of intracellular iron transport or iron regulation systems.

The convergence is particularly apparent at the mitochondria where four mutants (*Δimg2*, *Δmtm1*, *Δtom5* and *ΔYCR024c*) as well as control mutant *Δggc1* (formerly *Δyhm1*) exhibit high FOB and high ferrous uptake (Table 2). Three of the corresponding proteins are involved in mitochondrial protein biosynthesis or protein import. *Img2p* is a constituent of mitochondrial ribosome complex. *YCR024c* encodes a mitochondrial protein with asparaginyl-tRNA synthetase activity (LANDRIEU et al. 1997). Disruption of either gene generates a petite phenotype, although why deletion also generates this particular iron phenotype is not clear. *Tom5p* is part of the mitochondria outer membrane translocase complex and may serve as a functional link between the outer membrane receptors and the general import pore of the mitochondria (DIETMEIER et al. 1997). A role for this protein in the import of proteins involved in Fe-S cluster and/or heme cannot be excluded. The effect of *Tom5p* on cellular iron uptake is likely to be post-transcriptional, since disruption of the corresponding genes did not significantly alter the level of *FET3* and *SIT1* transcripts (data not shown). The corresponding protein for the other mutant in this group, *Mtm1p* is a mitochondrial carrier protein

involved in activation of Sod2 (LUK et al. 2003). The *Δmtm1* mutant was shown to accumulate iron in the mitochondria (LUK et al. 2003). Overall the phenotype of *Δmtm1* is very similar to that of strains defective in mitochondrial Fe-S cluster assembly *ssq1*, *nfs1*, and the control mutant strain *ggc1* (KNIGHT et al. 1998; LESUISSE et al. 2004; LI et al. 1999). This convergence of high FOB uptake and high ferrous uptake phenotypes in strains with mutations of genes encoding mitochondrial proteins underscores the importance of this organelle in cellular iron homeostasis and lends weight to our hypothesis (SANTOS et al. 2003) that a mitochondrial Fe-S cluster (that could be sensitive to oxidative stress especially by superoxides) performs a regulatory function in a signal transduction chain from the mitochondria to the cytosol to inform the cell of iron status. The majority (21) of the high FOB mutants with a defect in ferrous uptake had low ferrous uptake. This reciprocal phenotype convergence (high FOB, low ferrous uptake) was particularly noticeable in mutants whose corresponding proteins are located in, or involved with the secretory/vacuole system and the nucleus. The secretory/vacuolar mutants include *Δpep7*, *Δrav1*, *Δvps9*, *Δvam6*, *Δvma10*, and *Δvma13*. The low ferrous uptake of *Δrav1* and *Δvps9* mutants could be suppressed by the addition of copper to the growth media, in a manner identical to the control mutants *Δccc2* and *Δatx1*. Rav1p is involved in the regulation of vacuolar acidification and Vps9 is a guanine nucleotide exchange factor involved in vacuolar protein transport (HAMA et al. 1999). Although the low ferrous uptake phenotype of *Δvam6*, *Δvma10*, and *Δvma13* cannot be corrected by addition of copper to the growth media all three corresponding proteins are essential in vacuolar acidification. Vma6p and Vma10p are subunits of the H(+)-ATPase (BAUERLE et al. 1993; SUPEKOVA et al. 1995), and Vma13p is required for H(+)-ATPase assembly. These data support the idea that a functional vacuole is required for normal iron and copper cellular homeostasis (DAVIS-KAPLAN et al. 2004; SZCZYPKA et al. 1997), when the vacuole is dysfunctional ferrous uptake is diminished and the increase in FOB uptake is likely the result of a compensatory regulatory system.

The nucleus was also a site for reciprocal convergence of high FOB and low ferrous uptake for mutants *Δtup1*, *Δcyc8*, *Δmed1*, *Δssn3*, and *Δtaf1* (Table 2). The corresponding proteins all mediate transcription. We previously showed that the Tup1/Cyc8 general repressor complex was involved in iron uptake regulation, with preferential effects on derepressing the siderophore uptake pathway (LESUISSE et al. 2001). At this stage, it is not possible

to discriminate between factors that directly mediate transcription of the “iron regulon” genes and those that could act more indirectly. However, the copper correction of the low ferrous uptake of the *Δmed1* mutant might suggest that the corresponding protein mediates its effect on the genes encoding copper transport/distribution proteins.

Finally in this statistical analysis, one mutant had a distinct phenotype of low FOB uptake and low ferrous uptake. That mutant was *Δaft1*, the well-characterized iron regulatory transcription factor (YAMAGUCHI-IWAI et al. 1995). The uniqueness of this mutant phenotype from a primary screen of over 4847 mutants underscores the critical role Aft1p plays in yeast iron homeostasis.

Phenotypic categories and iron distribution: The initial screen identified many mutant strains of yeast with increased activity for iron uptake from FOB. The increased FOB uptake could be a regulatory consequence of cellular iron starvation occurring during growth (phenotypic category I). Alternatively, it could result from specific effects that increase siderophore transport into cells (phenotypic category II). Finally, increased FOB uptake activity could result from a general perturbation of iron sensing and iron regulation (phenotypic category III). We next evaluated examples of knockout mutants from each phenotypic category in terms of their intracellular iron distribution following iron loading with FOB as an iron source (Table 3). The results show that iron distribution was abnormal for mutants from each category, with proportionately decreased mitochondrial accumulation of iron. In the *Δvma10* mutant (category I), biogenesis of the vacuolar ATPase is disrupted. The iron phenotype was characterized by impaired ferrous transport and increased FOB uptake activity. When the cells were loaded with iron from FOB, cell associated iron was increased as expected. However, mitochondrial iron was not proportionately increased. In the *Δgga2* mutant (category II), the FOB uptake was specifically induced with no alteration of reductase or ferrous transport. The *Δgga2* mutant had the additional phenotype of accumulating colored iron siderophore complexes indicating a problem in dissociating them or distributing them intracellularly (see above). Following iron loading from FOB, cellular iron was increased, and again, mitochondrial iron was not proportionately increased. In mutants of *TOM5*, *POR1*, *FMCI*, *IMG2* (category II), mitochondrial functions are disrupted to varying degrees and in pleiotropic manner. Reductive and FOB transport were induced, but again, following loading with iron from FOB, mitochondrial iron accumulation was not proportionately increased. The implication of all these

results is that cellular iron uptake and mitochondrial iron accumulation from FOB are subject to separate controls. Many of the mutations that impacted on cellular iron uptake, inducing FOB transport activity, did not induce mitochondrial deposition of the iron. This is in contrast to the phenotype of Fe-S cluster assembly mutants in which induction of FOB uptake activity and mitochondrial iron accumulation are salient features. Two mutants (category III) were examined which did not adhere to the pattern described above. Instead, they exhibited increased iron transport activities (reductase, ferrous transport and FOB transport), but following loading with iron *via* FOB, they accumulated mitochondrial iron in proportion to cellular iron, and so the ratio of these compartmental accumulations was not altered (Table 3). YLL029w and YGL220w encode uncharacterized ORFs. The corresponding proteins are reported to be cytoplasmic, and it is interesting to speculate that they may coordinately control cytoplasmic and mitochondrial iron distribution. YLL029w may be especially interesting to study further, since the corresponding mutant accumulated FOB as its undissociated form (see above). One important question that arises from the analysis of iron distribution in strains showing increased FOB uptake is indeed related to the cellular location where iron dissociation from the siderophore takes place. Is iron necessarily released from the siderophore before entering the mitochondria, or is there some pathway for siderophore uptake and use by the mitochondria itself? Our iron distribution studies do not answer to this question. Mutants known to accumulate iron by the reductive pathway followed by iron deposition in the mitochondria ($\Delta yfh1$, $\Delta atm1$ etc...) also accumulate iron from siderophores (LESUISSE et al. 2001), but the intracellular distribution of this siderophore-iron was never investigated. The cells deleted for YLL029w accumulated FOB in an undissociated form (whole cells were colored after growth with FOB), and showed increased iron in their mitochondria compared to wild-type cells (Table 3), but further work would be required to determine if part of the intracellular FOB could be found undissociated inside the mitochondria. Mitochondria are intrinsically more pigmented than whole cells, and thus accumulation of the siderophore pigment into this organelle is less obvious to determine than in whole cells. We are currently working on these questions related to the intracellular dissociation of siderophores.

General conclusion and caveats: This study of the entire set of viable haploid deletion strains of *S. cerevisiae* from the Euroscarf collection revealed a huge number of genes with involvement in cellular

iron homeostasis. In the initial screen for FOB uptake, more than 10% of the mutants (570 strains) showed altered activity compared to the wild-type strain. A subset with reproducibly abnormal phenotypes was selected and analyzed as homozygous diploids (197 strains including 79 with mutations in *COX*, *ATP* and *MRP(L)* genes which will be presented separately). Some strains affected in iron metabolism probably passed through the net of our successive screens for several reasons. First, all the strains that did not show altered iron uptake in the first screen were not studied further; thus, errors in measuring uptake values in the first screen may have led to discarding some potentially interesting strains. Second, our screen was more sensitive at detecting high FOB uptake strains than low FOB uptake strains (for technical reasons related to the specific activity of ^{55}Fe we used). Finally, a large number of mutants showed an unstable phenotype, with progressive attenuation of the high uptake phenotype. Probably this was due to accumulation of extragenic suppressor mutations. In addition, it is important to note that only the strains considered as viable in the Euroscarf collection were screened. Curiously, mutants with defective Fe-S cluster assembly were not selected here. Some were classified as essential genes (e.g. *YFH1*, *ATM1*) and others were missed perhaps due to masking of the phenotype by suppressors (e.g. *SSQ1*). Despite all these limitations, in this study a large number of genes were implicated in iron metabolism for the first time. These included genes encoding predicted proteins located in the plasma membrane, cytoplasm, secretory pathway, nucleus and mitochondria. Future work will endeavor to determine which of these affect iron metabolism directly via transport or sequestration of iron and which affect iron metabolism indirectly via signals or protein trafficking.

A special feature of the screen is the measurement of distinct uptake systems. One of the uptake systems (reductive) is active during growth in the usual media and its activity reflects iron regulation and the history of iron exposure during growth of the cells. The other system (siderophore) is generally not used during growth in customary media, because this media do not contain siderophores. However, activity for siderophore uptake is also responsive to iron homeostasis. Clustering of the uptake data makes possible distinction between mutants with altered trafficking of specific components or mutants with generally altered iron metabolism.

ACKNOWLEDGMENTS

This work was supported by grants from the French Ministère de la Recherche (Programme de

Recherches Fondamentales en Microbiologie, Maladies Infectieuses et Parasitaires and Réseau Infection Fongique) and from the Association pour la Recherche sur le Cancer (ARC 5439 and 4396). This work was supported by National Institutes of Health Grant DK53953 (to A.D.). We thank David Dancis for technical support and we thank Rachel Weinstein of the University of Pennsylvania Biostatistics Analysis Center for assistance with the statistical analysis.

LITERATURE CITED

- BAUERLE, C., M. N. HO, M. A. LINDORFER and T. H. STEVENS, 1993 The *Saccharomyces cerevisiae* VMA6 gene encodes the 36-kDa subunit of the vacuolar H(+)-ATPase membrane sector. *J Biol Chem* **268**: 12749-57.
- BLAISEAU, P. L., E. LESUISSE and J. M. CAMADRO, 2001 Aft2p, a novel iron-regulated transcription activator that modulates, with Aft1p, intracellular iron use and resistance to oxidative stress in yeast. *J. Biol. Chem.* **276**: 34221-34226.
- CAMADRO, J. M., F. THOME, N. BROUILLET and P. LABBE, 1994 Purification and properties of protoporphyrinogen oxidase from the yeast *Saccharomyces cerevisiae*. Mitochondrial location and evidence for a precursor form of the protein. *J. Biol. Chem.* **269**: 32085-32091.
- CRISP, R. J., A. POLLINGTON, C. GALEA, S. JARON, Y. YAMAGUCHI-IWAI et al., 2003 Inhibition of heme biosynthesis prevents transcription of iron uptake genes in yeast. *J Biol Chem* **278**: 45499-506. Epub 2003 Aug 19.
- DANCIS, A., R. D. KLAUSNER, A. G. HINNEBUSCH and J. G. BARRIOCANAL, 1990 Genetic evidence that ferric reductase is required for iron uptake in *Saccharomyces cerevisiae*. *Mol. Cell. Biol.* **10**: 2294-2301.
- DANCIS, A., D. G. ROMAN, G. J. ANDERSON, A. G. HINNEBUSCH and R. D. KLAUSNER, 1992 Ferric reductase of *Saccharomyces cerevisiae*: molecular characterization, role in iron uptake, and transcriptional control by iron. *Proc. Natl. Acad. Sci. USA* **89**: 3869-73.
- DANCIS, A., D. S. YUAN, D. HAILE, C. ASKWITH, D. EIDE et al., 1994 Molecular characterization of a copper transport protein in *S. cerevisiae*: an unexpected role for copper in iron transport. *Cell* **76**: 393-402.
- DAVIS-KAPLAN, S. R., D. M. WARD, S. L. SHIFLETT and J. KAPLAN, 2004 Genome-wide analysis of iron-dependent growth reveals a novel yeast gene required for vacuolar acidification. *J Biol Chem* **279**: 4322-9. Epub 2003 Nov 21.
- DE HOON, M. J., S. IMOTO, J. NOLAN and S. MIYANO, 2004 Open source clustering software. *Bioinformatics* **20**: 1453-4. Epub 2004 Feb 10.
- DIETMEIER, K., A. HONLINGER, U. BOMER, P. J. DEKKER, C. ECKERSKORN et al., 1997 Tom5 functionally links mitochondrial preprotein receptors to the general import pore. *Nature* **388**: 195-200.
- DIX, D., J. BRIDGHAM, M. BRODERIUS and D. EIDE, 1997 Characterization of the FET4 protein of yeast. Evidence for a direct role in the transport of iron. *J. Biol. Chem.* **272**: 11770-11777.
- EISEN, M. B., P. T. SPELLMAN, P. O. BROWN and D. BOTSTEIN, 1998 Cluster analysis and display of genome-wide expression patterns. *Proc. Natl. Acad. Sci. USA* **95**: 14863-14868.
- FOURY, F., and D. TALIBI, 2001 Mitochondrial control of iron homeostasis. A genome wide analysis of gene expression in a yeast frataxin-deficient strain. *J. Biol. Chem.* **276**: 7762-7768.
- GEORGATSOU, E., and D. ALEXANDRAKI, 1994 Two distinctly regulated genes are required for ferric reduction, the first step of iron uptake in *Saccharomyces cerevisiae*. *Mol. Cell. Biol.* **14**: 3065-3073.
- GEORGATSOU, E., L. A. MAVROGIANNIS, G. S. FRAGIADAKIS and D. ALEXANDRAKI, 1997 The yeast Fre1p/Fre2p cupric reductases facilitate copper uptake and are regulated by the copper-modulated Mac1p activator. *J. Biol. Chem.* **272**: 13786-13792.
- GERBER, J., K. NEUMANN, C. PROHL, U. MUHLENHOFF and R. LILL, 2004 The yeast scaffold proteins Isu1p and Isu2p are required inside mitochondria for maturation of cytosolic Fe/S proteins. *Mol Cell Biol* **24**: 4848-57.
- HAAS, H., 2003 Molecular genetics of fungal siderophore biosynthesis and uptake: the role of siderophores in iron uptake and storage. *Appl Microbiol Biotechnol* **62**: 316-30. Epub 2003 May 21.
- HAMA, H., E. A. SCHNIEDERS, J. THORNER, J. Y. TAKEMOTO and D. B. DEWALD, 1999 Direct involvement of phosphatidylinositol 4-phosphate in secretion in the yeast *Saccharomyces cerevisiae*. *J Biol Chem* **274**: 34294-300.

- HEYMANN, P., J. F. ERNST and G. WINKELMANN, 1999 Identification of a fungal triacetylfusarinine C siderophore transport gene (*TAFI*) in *Saccharomyces cerevisiae* as a member of the major facilitator superfamily. *Biometals* **12**: 301-306.
- HEYMANN, P., J. F. ERNST and G. WINKELMANN, 2000 A gene of the major facilitator superfamily encodes a transporter for enterobactin (Enb1p) in *Saccharomyces cerevisiae*. *Biometals* **13**: 65-72.
- JENSEN, L. T., R. J. SANCHEZ, C. SRINIVASAN, J. S. VALENTINE and V. C. CULOTTA, 2004 Mutations in *Saccharomyces cerevisiae* Iron-Sulfur Cluster Assembly Genes and Oxidative Stress Relevant to Cu,Zn Superoxide Dismutase. *J Biol Chem* **279**: 29938-43. Epub 2004 Apr 23.
- KARTHIKEYAN, G., L. K. LEWIS and M. A. RESNICK, 2002 The mitochondrial protein frataxin prevents nuclear damage. *Hum Mol Genet* **11**: 1351-62.
- KATZMANN, D. J., G. ODORIZZI and S. D. EMR, 2002 Receptor downregulation and multivesicular-body sorting. *Nat Rev Mol Cell Biol* **3**: 893-905.
- KIM, Y., C. W. YUN and C. C. PHILPOTT, 2002 Ferrichrome induces endosome to plasma membrane cycling of the ferrichrome transporter, Arn1p, in *Saccharomyces cerevisiae*. *Embo J* **21**: 3632-42.
- KNIGHT, S., E. LESUISSE, R. STEARMAN, R. D. KLAUSNER and A. DANCIS, 2002 Reductive iron uptake by *Candida albicans*: role of copper, iron and the *TUPI* regulator. *Microbiol.* **148**: 29-40.
- KNIGHT, S. A., S. LABBE, L. F. KWON, D. J. KOSMAN and D. J. THIELE, 1996 A widespread transposable element masks expression of a yeast copper transport gene. *Genes Dev* **10**: 1917-29.
- KNIGHT, S. A., N. B. SEPURI, D. PAIN and A. DANCIS, 1998 Mt-Hsp70 homolog, Ssc2p, required for maturation of yeast frataxin and mitochondrial iron homeostasis. *J. Biol. Chem.* **273**: 18389-18393.
- KOHRER, K., and H. DOMDEY, 1991 Preparation of high molecular weight RNA. *Methods Enzymol.* **194**: 398-405.
- KOSMAN, D. J., 2003 Molecular mechanisms of iron uptake in fungi. *Mol. Microbiol.* **47**: 1185-1197.
- LANDRIEU, I., M. VANDENBOL, M. HARTLEIN and D. PORTETELLE, 1997 Mitochondrial asparaginyl-tRNA synthetase is encoded by the yeast nuclear gene YCR24c. *Eur J Biochem* **243**: 268-73.
- LESUISSE, E., P. L. BLAISEAU, A. DANCIS and J. M. CAMADRO, 2001 Siderophore uptake and use by the yeast *Saccharomyces cerevisiae*. *Microbiol.* **147**: 289-298.
- LESUISSE, E., and P. LABBE, 1989 Reductive and non-reductive mechanisms of iron assimilation by the yeast *Saccharomyces cerevisiae*. *J. Gen. Microbiol.* **135**: 257-263.
- LESUISSE, E., E. R. LYVER, S. A. KNIGHT and A. DANCIS, 2004 Role of *YHM1*, encoding a mitochondrial carrier protein, in iron distribution of yeast. *Biochem. J.* **378**: 599-607.
- LESUISSE, E., R. SANTOS, B. F. MATZANKE, J. M. CAMADRO and A. DANCIS, 2003 Iron use for heme synthesis is under control of the yeast frataxin homologue (Yfh1). *Hum. Mol. Genet.* **12**: 879-889.
- LESUISSE, E., M. SIMON-CASTERAS and P. LABBE, 1998 Siderophore-mediated iron uptake in *Saccharomyces cerevisiae*: the *SITI* gene encodes a ferrioxamine B permease that belongs to the major facilitator superfamily. *Microbiol.* **144**: 3455-3462.
- LI, J., M. KOGAN, S. A. KNIGHT, D. PAIN and A. DANCIS, 1999 Yeast mitochondrial protein, Nfs1p, coordinately regulates iron-sulfur cluster proteins, cellular iron uptake, and iron distribution. *J. Biol. Chem.* **274**: 33025-33034.
- LUK, E., M. CARROLL, M. BAKER and V. C. CULOTTA, 2003 Manganese activation of superoxide dismutase 2 in *Saccharomyces cerevisiae* requires MTM1, a member of the mitochondrial carrier family. *Proc Natl Acad Sci U S A* **100**: 10353-7. Epub 2003 Jul 30.
- RAGUZZI, F., E. LESUISSE and R. R. CRICHTON, 1988 Iron storage in *Saccharomyces cerevisiae*. *FEBS Lett.* **231**: 253-258.
- RUTHERFORD, J. C., S. JARON, E. RAY, P. O. BROWN and D. R. WINGE, 2001 A second iron-regulatory system in yeast independent of Aft1p. *Proc. Natl. Acad. Sci. USA* **98**: 14322-14327.
- SAMBROOK, J., E. F. FRITSCH and T. MANIATIS, 1989 *Molecular cloning: a laboratory manual*. Cold Spring Harbor Laboratory, Cold Spring, N.Y.
- SANTOS, R., A. DANCIS, D. EIDE, J. M. CAMADRO and E. LESUISSE, 2003 Zinc suppresses the iron-accumulation phenotype of *Saccharomyces cerevisiae* lacking the yeast frataxin homologue (Yfh1). *Biochem. J.* **375**: 247-254.

- SEOL, J. H., A. SHEVCHENKO and R. J. DESHAIES, 2001 Skp1 forms multiple protein complexes, including RAVE, a regulator of V-ATPase assembly. *Nat Cell Biol* **3**: 384-91.
- SHATWELL, K. P., A. DANCIS, A. R. CROSS, R. D. KLAUSNER and A. W. SEGAL, 1996 The FRE1 ferric reductase of *Saccharomyces cerevisiae* is a cytochrome b similar to that of NADPH oxidase. *J Biol Chem* **271**: 14240-4.
- STEARMAN, R., D. S. YUAN, Y. YAMAGUCHI-IWAI, R. D. KLAUSNER and A. DANCIS, 1996 A permease-oxidase complex involved in high-affinity iron uptake in yeast. *Science* **271**: 1552-1557.
- SUPEKOVA, L., F. SUPEK and N. NELSON, 1995 The *Saccharomyces cerevisiae* VMA10 is an intron-containing gene encoding a novel 13-kDa subunit of vacuolar H(+)-ATPase. *J Biol Chem* **270**: 13726-32.
- SZCZYPKA, M. S., Z. ZHU, P. SILAR and D. J. THIELE, 1997 *Saccharomyces cerevisiae* mutants altered in vacuole function are defective in copper detoxification and iron-responsive gene transcription. *Yeast* **13**: 1423-35.
- URBANOWSKI, J. L., and R. C. PIPER, 1999 The iron transporter Fth1p forms a complex with the Fet5 iron oxidase and resides on the vacuolar membrane. *J. Biol. Chem.* **274**: 38061-38070.
- VOZZA, A., E. BLANCO, L. PALMIERI and F. PALMIERI, 2004 Identification of the mitochondrial GTP/GDP transporter in *Saccharomyces cerevisiae*. *J Biol Chem* **279**: 20850-7. Epub 2004 Mar 3.
- YAMAGUCHI-IWAI, Y., A. DANCIS and R. D. KLAUSNER, 1995 *AFT1*: a mediator of iron regulated transcriptional control in *Saccharomyces cerevisiae*. *EMBO J.* **14**: 1231-1239.
- YAMAGUCHI-IWAI, Y., R. STEARMAN, A. DANCIS and R. D. KLAUSNER, 1996 Iron-regulated DNA binding by the AFT1 protein controls the iron regulon in yeast. *EMBO J.* **15**: 3377-3384.
- YUAN, D. S., A. DANCIS and R. D. KLAUSNER, 1997 Restriction of copper export in *Saccharomyces cerevisiae* to a late Golgi or post-Golgi compartment in the secretory pathway. *J Biol Chem* **272**: 25787-93.
- YUN, C. W., T. FEREA, J. RASHFORD, O. ARDON, P. O. BROWN et al., 2000a Desferrioxamine-mediated iron uptake in *Saccharomyces cerevisiae*. Evidence for two pathways of iron uptake. *J. Biol. Chem.* **275**: 10709-10715.
- YUN, C. W., J. S. TIEDEMAN, R. E. MOORE and C. C. PHILPOTT, 2000b Siderophore-iron uptake in *Saccharomyces cerevisiae*. Identification of ferrichrome and fusarinine transporters. *J. Biol. Chem.* **275**: 16354-16359.

TABLE 1. Progressive loss, in successive screens, of the high FOB uptake phenotype in some haploid strains. The values indicate the rate of FOB uptake compared to wild type (= 1).

ORF	Gene	Screen 1	Screen 2	Screen 3	Screen 4
<i>YNL170W</i>	<i>YNL170W</i>	5.6	4.4	1.6	1.8
<i>YHR100C</i>	<i>YHR100C</i>	7.5	1.9	3	2.5
<i>YAL048C</i>	<i>GON1</i>	5.3	3.1	1.5	1
<i>YML088W</i>	<i>UFO1</i>	11.5	3	1.3	0.9
<i>YMR287C</i>	<i>MSU1</i>	5.7	0.9	0.9	nd
<i>YOR036W</i>	<i>PEP12</i>	5.6	2.2	2	1.5
<i>YOR123C</i>	<i>LEO1</i>	2.5	1.6	0.9	nd
<i>YOR141C</i>	<i>ARP8</i>	2.4	1.2	0.4	nd
<i>YDL198C</i>	<i>YHMI</i>	16.6	11.7	1.6	1.3
<i>YDR364C</i>	<i>CDC40</i>	9.1	2.1	1.0	1.6
<i>YKL155C</i>	<i>RSM22</i>	12.5	2.6	1.2	1
<i>YLR369W</i>	<i>SSQ1</i>	19.4	1.7	0.8	0.8
<i>YLR418C</i>	<i>CDC73</i>	8.6	4	2.9	1
<i>YNR010W</i>	<i>CSE2</i>	11.8	1.9	1.5	0.7
<i>YNR037C</i>	<i>RSM19</i>	5.9	2.9	0.7	0.5
<i>YPR160W</i>	<i>GPH1</i>	7.6	5.6	2.7	0.3
<i>YFL023W</i>	<i>BUD27</i>	6.9	5.8	1.3	0.7
<i>YCR024C</i>	<i>YCR024C</i>	8.9	2.5	1.1	1
<i>YCR071C</i>	<i>IMG2</i>	3.9	2	1.0	0.7
<i>YCR081W</i>	<i>SRB8</i>	9.8	4.5	1.6	0.6
<i>YGR063C</i>	<i>SPT4</i>	14.1	4	2.8	2.4
<i>YFL014W</i>	<i>HSP12</i>	12.1	4.9	1.5	0.4
<i>YPR133W</i>	<i>TOM5</i>	11.2	6.3	2.0	2.5
<i>YNL147W</i>	<i>LSM7</i>	3.8	3.6	1.5	1.2
<i>YGR257C</i>	<i>MTM1</i>	9.5	4.3	1.3	0.9

TABLE 2. GO proposed location of proteins corresponding to homozygous diploid mutants with high or low FOB uptake, ferrireductase activity, and ferrous uptake. Mutant FOB uptake defined as Low if mean value of three assays ≤ 0.6 x wild type, and defined as high if ≥ 1.8 x wild type. Mutant ferrireductase activity and ferrous uptake defined as High or Low if statistically different from wild type ($p < 0.05$). • control homozygous diploid mutant. † low ferrous uptake correctable by copper to wild type levels.

ORF	Standard Name	FOB	Fe Rdx	Ferrous	GO Cellular Component	GO Biological Process/ notes
Plasma Membrane						
<i>CTR1*</i>	<i>YPR124W</i>	High	High	Low†	Plasma membrane	Ion (Cu) transport
<i>FRE4</i>	<i>YNR060W</i>	High	ns	ns	Plasma membrane	Ion (Fe) transport
<i>SITI</i>	<i>YEL065W</i>	Low	ns	ns	Plasma membrane	Ion (Fe) transport
Cytoplasm						
	<i>YLL029W</i>	High	High	High	Cytoplasm	Unknown
<i>CYS4</i>	<i>YGR155W</i>	High	High	Low	Cytoplasm	Cysteine biosynthesis
<i>PEP7</i>	<i>YDR323C</i>	High	High	Low	Cytoplasm	Golgi to vacuole transport
<i>RAV1</i>	<i>YJR033C</i>	High	High	Low†	Cytoplasm	Vacuolar acidification
<i>VPS9</i>	<i>YML097C</i>	High	High	Low†	Cytoplasm	Protein-vacuolar targeting
<i>ATX1*</i>	<i>YNL259C</i>	High	High	Low†	Cytoplasm	Ion (Cu) transport
<i>APS3</i>	<i>YJL024C</i>	High	ns	ns	Cytoplasm	Golgi to vacuole transport
<i>RPS11A</i>	<i>YDR025W</i>	High	ns	ns	Cytoplasm	Protein biosynthesis
<i>CCR4</i>	<i>YAL021C</i>	High	Low	ns	Cytoplasm	Transcription regulator
<i>LSM1</i>	<i>YJL124C</i>	High	Low	ns	Cytoplasm	RNA processing
<i>PAT1</i>	<i>YCR077C</i>	High	Low	ns	Cytoplasm	RNA processing
Cytoplasm/secretory						
<i>BRO1</i>	<i>YPL084W</i>	High	High	ns	Cytoplasm/endosome	Signal transduction/ vacuolar transport
<i>SNF7</i>	<i>YLR025W</i>	High	High	ns	Cytoplasm/endosome	Endosome to vacuole transport
<i>VPS20</i>	<i>YMR077C</i>	High	High	ns	Cytoplasm/endosome	Endosome to vacuole transport
<i>CDC50</i>	<i>YCR094W</i>	High	High	ns	Endosome	Cell polarity / cell cycle
<i>VPS25</i>	<i>YJR102C</i>	High	High	ns	Endosome	Protein-vacuolar targeting
<i>VPS28</i>	<i>YPL065W</i>	High	High	ns	Endosome	Protein-vacuolar targeting
<i>VPS36</i>	<i>YLR417W</i>	High	High	ns	Endosome	Protein-vacuolar targeting
<i>VMA10</i>	<i>YHR039C-B</i>	High	High	Low	Vacuole	Vacuolar acidification
<i>VMA13</i>	<i>YPR036W</i>	High	High	Low	Vacuole	Vacuolar acidification
<i>VMA6</i>	<i>YLR447C</i>	High	High	Low	Vacuole	Vacuolar acidification
<i>VAM6</i>	<i>YDL077C</i>	High	ns	ns	Vacuole	Vacuolar biogenesis
<i>ARF1</i>	<i>YDL192W</i>	High	High	Low	Cytoplasm/golgi	ER to golgi transport
<i>PEP12</i>	<i>YOR036W</i>	High	High	Low	Golgi	Golgi to vacuole transport
<i>CCC2*</i>	<i>YDR270</i>	High	High	Low†	Golgi	Ion (Cu) transport
<i>GGA2</i>	<i>YHR108W</i>	High	ns	ns	Golgi	Golgi to vacuole transport
<i>VPS4</i>	<i>YPR173C</i>	High	High	ns	Cytoplasm/ER	Endosome to vacuole transport
<i>VPS64</i>	<i>YDR200C</i>	High	High	Low	Cytoplasm/ER	Protein-vacuolar targeting
<i>PKR1</i>	<i>YMR123W</i>	High	High	Low†	ER	Unknown
<i>VMA21</i>	<i>YGR105</i>	High	High	Low	ER	Protein complex assembly
Cytoplasm/nucleus						
<i>PPZ1</i>	<i>YML016C</i>	High	High	High	Cytoplasm/nucleus	ion (Na) homeostasis
<i>BUD32</i>	<i>YGR262C</i>	High	High	ns	Cytoplasm/nucleus	Bud site selection
<i>VID28</i>	<i>YIL017C</i>	High	High	ns	Cytoplasm/nucleus	Regulation of gluconeogenesis

	<i>YGL220</i>	High	ns	ns	Cytoplasm/nucleus	unknown
<i>FYVI</i>	<i>YDR024W</i>	High	ns	Low	Cytoplasm/nucleus	Unknown - Dubious ORF
<i>DEG1</i>	<i>YFL001W</i>	Low	High	ns	Cytoplasm/nucleus	RNA processing
<i>HSP12</i>	<i>YFL014W</i>	Low	ns	ns	Cytoplasm/nucleus	Stress response
<i>RCS1(AFT1)</i>	<i>YGL071W</i>	Low	ns	Low	Cytoplasm/nucleus	Transcription regulator
<i>SPT4</i>	<i>YGR063C</i>	High	High	High	Nucleus	RNA elongation
<i>CDC73</i>	<i>YLR418C</i>	High	High	ns	Nucleus	RNA elongation
<i>NPL6</i>	<i>YMR091</i>	High	High	Low	Nucleus	Protein-nucleus import
<i>SRB8</i>	<i>YCR081W</i>	High	High	Low	Nucleus	Transcription regulator
<i>LSM7</i>	<i>YNL147W</i>	High	ns	ns	Nucleus	mRNA splicing
<i>ARP5</i>	<i>YNL059C</i>	High	ns	ns	Nucleus	Protein-vacuolar targeting
<i>TUP1</i>	<i>YCR084C</i>	High	ns	Low	Nucleus	Transcription regulator
<i>LSM6</i>	<i>YDR378C</i>	High	Low	ns	Nucleus	RNA processing
<i>SRB5</i>	<i>YGR104CC</i>	High	Low	ns	Nucleus	RNA elongation
<i>SSN8</i>	<i>YNL025C</i>	High	Low	ns	Nucleus	Transcription regulator
<i>CYC8</i>	<i>YBR112C</i>	High	Low	Low	Nucleus	Transcription regulator
<i>MED1</i>	<i>YPR070W</i>	High	Low	Low†	Nucleus	Transcription
<i>SSN3</i>	<i>YPL042C</i>	High	Low	Low	Nucleus	Transcription regulator
<i>TAF14</i>	<i>YPL129W</i>	High	Low	Low	Nucleus	Transcription
<i>EBS1</i>	<i>YDR206W</i>	Low	ns	ns	Nucleus	Telomere maintenance
Mitochondrion						
<i>IMG2</i>	<i>YCR071C</i>	High	High	High	Mitochondrion	Protein biosynthesis
<i>MTM1</i>	<i>YGR257C</i>	High	High	High	Mitochondrion	ion (Mn) transport
<i>TOM5</i>	<i>YPR133W-A</i>	High	High	High	Mitochondrion	Protein import
	<i>YCR024C</i>	High	High	High	Mitochondrion	Protein biosynthesis
<i>GGC1*</i>	<i>YDL198C</i>	High	High	High	Mitochondrion	transport / ion (Fe) homeostasis
<i>FMC1</i>	<i>YIL098C</i>	High	High	ns	Mitochondrion	Protein complex assembly
<i>LPD1</i>	<i>YFL018C</i>	High	High	ns	Mitochondrion	Pyruvate dehydrogenase
<i>MRS1</i>	<i>YIR021W</i>	High	High	ns	Mitochondrion	Intron splicing
<i>POR1</i>	<i>YNL055C</i>	High	High	ns	Mitochondrion	Respiration / iron transport
<i>RSM19</i>	<i>YNR037C</i>	High	High	ns	Mitochondrion	Protein biosynthesis
<i>YME1</i>	<i>YPR024W</i>	High	High	ns	Mitochondrion	Mitochondrion biogenesis
<i>SSQ1*</i>	<i>YLR369W</i>	High	High	Low†	Mitochondrion	Ion (Fe) homeostasis
<i>GRX5</i>	<i>YPL059W</i>	High	ns	ns	Mitochondrion	stress response
<i>HEM14</i>	<i>YER014W</i>	High	Low	ns	Mitochondrion	Heme biosynthesis
Other						
<i>MMR1</i>	<i>YLR190W</i>	High	High	ns	Bud neck	Unknown
<i>RCY1</i>	<i>YJL204C</i>	High	High	ns	Site of growth	Endocytosis
Unknown						
<i>DIA2</i>	<i>YOR080W</i>	High	High	ns	Unknown	Invasive growth
	<i>YGR064W</i>	High	High	ns	Unknown	Unknown. Overlap with SPT4
	<i>YHR100C</i>	High	High	ns	Unknown	Unknown
	<i>YLR358C</i>	High	High	ns	Unknown	Unknown. Overlap with RSC2
<i>VPS63</i>	<i>YLR261C</i>	High	High	Low	Unknown	Unknown. Overlap with YPT6
	<i>YDR199W</i>	High	ns	ns	Unknown	Unknown. Dubious ORF
	<i>YKL097C</i>	High	ns	ns	Unknown	Unknown. Dubious ORF
	<i>YLL030C</i>	High	ns	ns	Unknown	Unknown. Dubious ORF
<i>BUD25</i>	<i>YER014C-A</i>	High	Low	ns	Unknown	Unknown. Overlap with HEM14

TABLE 3. Intracellular iron distribution in selected strains belonging to different phenotypic categories. Cells were grown overnight in YPD medium containing $10 \mu\text{M } ^{55}\text{Fe-FOB}$, harvested in late exponential phase of growth, and fractionated to determine the amount of iron in the soluble and mitochondrial fractions. Data from one experiment.

strain	phenotype category	Whole cells (pmol Fe/OD)	Mitochondria (pmol Fe/mg)	Soluble (pmol Fe/mg)	Mito/soluble
WT		38	7240	1265	5.72
<i>VMA10</i>	I	555	21265	31015	0.69
<i>GGA2</i>	II	1003	29943	49123	0.61
<i>BUD25</i>	II	80	7161	4076	1.76
<i>TOM5</i>	III	249	19898	24851	0.80
<i>POR1</i>	III	112	14732	7955	1.85
<i>FMCI</i>	III	87	5865	5325	1.10
<i>IMG2</i>	III	257	54152	34422	1.57
<i>YGL220_w</i>	III	170	22890	5813	3.94
<i>YLL029_w</i>	III	167	30457	7323	4.16

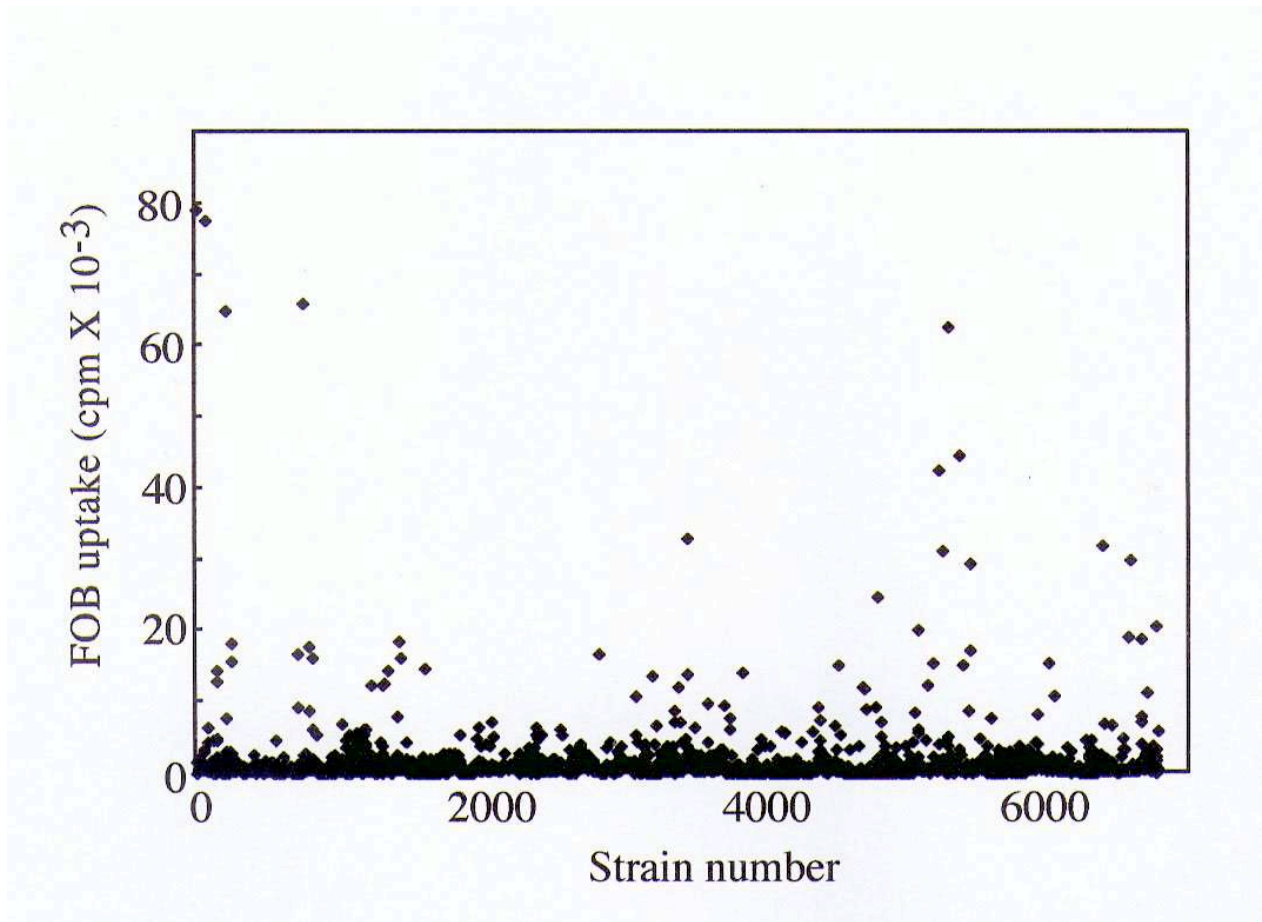


Figure 1: The complete haploid knockout collection from EUROSCARF was assayed for FOB uptake. Data for strains in sequentially numbered wells in microtiter plates (x-axis) were plotted as a scattergram against uptake data in cpm (y-axis). Due to the presence of numerous empty wells on the assay plates, the number of assays (more than 7000) exceeded the number of knockout strains (4847). The value for the wild type was 1009 cpm.

Colony/Strain FOB uptake

	BY4741 (WT)	1
	YLL029w	4
	TIM18	6.4
	GGA2	9.3
	YGR064w	4.3
	CIK1	2.6
	YGR063c	2.4
	GGC1/YHM1	3.4
	AFT1up	10.2
	ARF1	8.5

Figure 2. Colonies of haploid mutant strains that accumulated undissociated FOB. The indicated strains were spotted on a YPD-agar plate containing 50 μ M FOB and allowed to grow for 3 days at 30°C. The appearance of the colonies was recorded (left column). The rate of FOB uptake by each mutant was measured independently as described in Methods. Values for each mutant were reported as n-fold the value of the wild-type FOB uptake rate (right column).

1: FeRed - Cu	4: ENB	7: FOB
2: FeRed + Cu	5: Fe(II) - Cu	8: FCH
3: FeRed + BPS	6: Fe(II) + Cu	9: TAF

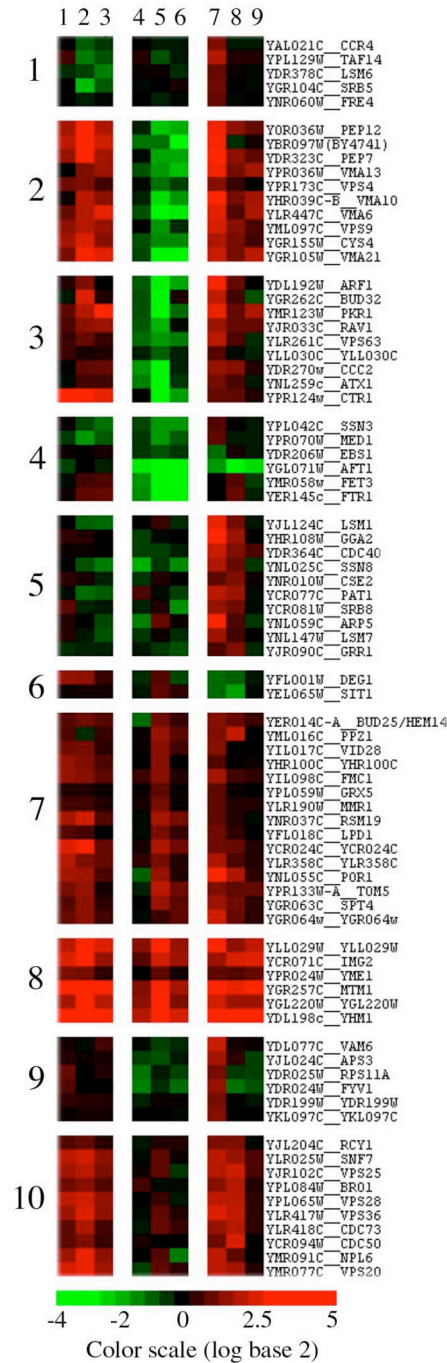


Figure 3. Clustering of data for ferric reductase, iron uptake from ferrous salts, and iron uptake from various siderophores by diploid knockout strains. FeRed, ferric reductase activity (in copper deficient (-Cu), copper replete (+ Cu) or iron deficient (BPS) conditions); Fe(II), ferrous uptake activity; ENB, FOB, FCH, TAF, siderophore uptake activity (from enterobactin, ferrioxamine B, ferrichrome and triacetylfulvarinine C, respectively). Results are expressed (according to the color scale) in log base 2 as the ratio mutant/wild type. Means from 4 experiments.

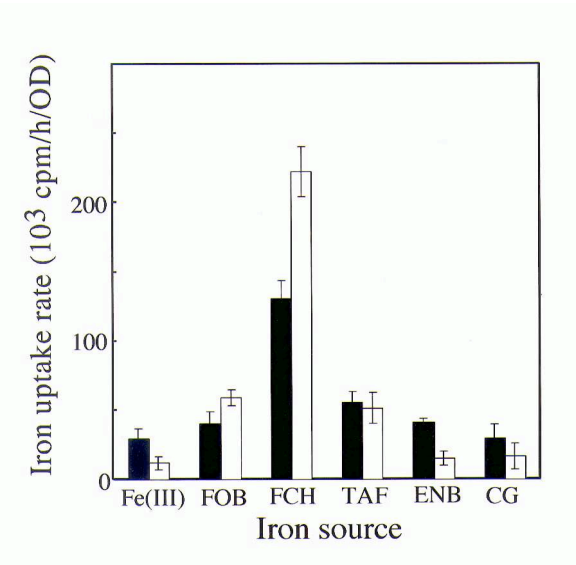


Figure 4. Iron uptake rates from various iron sources by wild-type (closed columns) or $\Delta fre1\Delta fre2$ (open columns) cells of *S. cerevisiae* (S150-2B). Cells were incubated for 30 min in complete (YPD) medium containing 1 μM of the indicated iron source (as ^{55}Fe) before washing and determining intracellular iron. Fe(III), ferric citrate; FOB, ferrioxamine B; FCH, ferrichrome; TAF, triacetylfusarinine C; ENB, enterobactin; CG, coprogen. Mean \pm SD from 4 experiments.

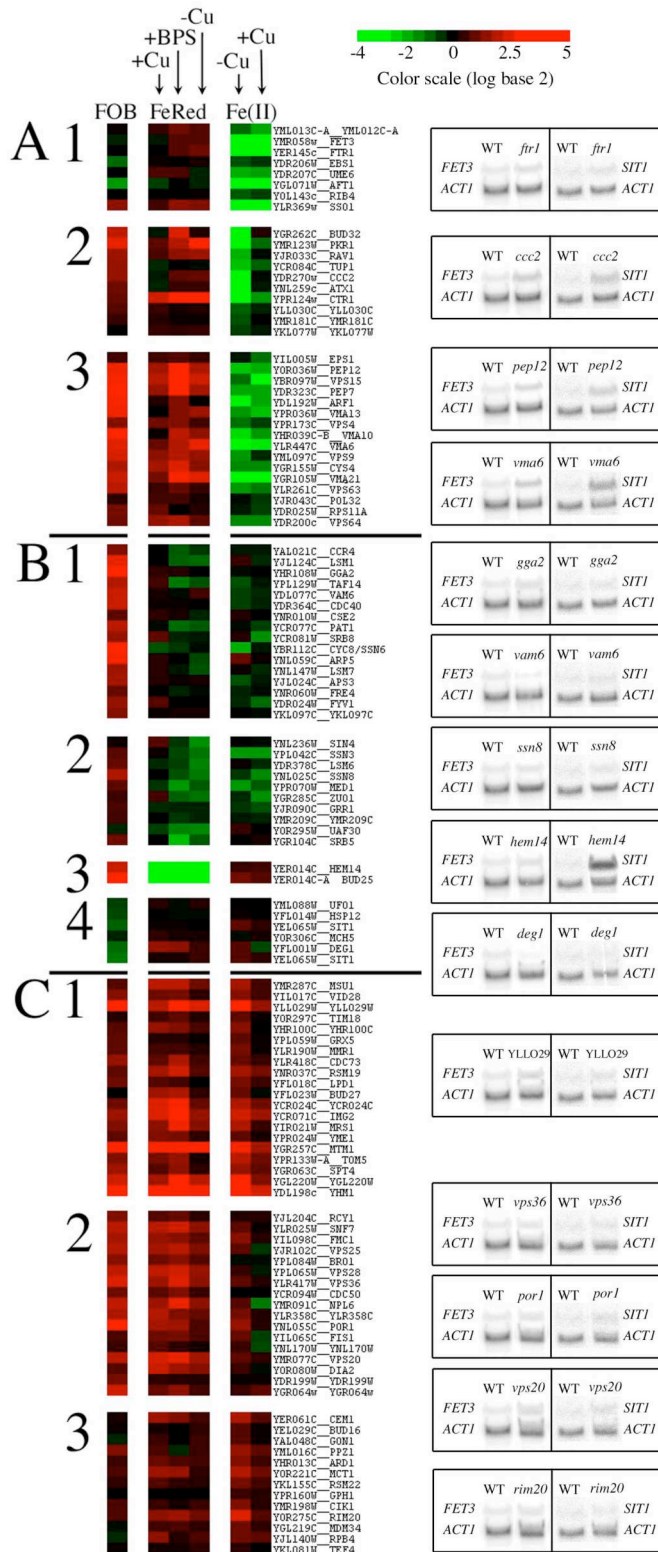


Figure 5. Clustering of homozygous mutants with similar phenotypes for FOB iron uptake, ferric reductase, and ferrous iron uptake (left panel). Nodes of similar mutants were further grouped into three categories with different uptake signatures: A with low ferrous uptake, B with high or low FOB uptake, C with high FOB uptake, ferric reductase, and ferrous uptake. For each node, representative mutants were selected, mRNA was isolated and tested by Northern blotting for *SITI1* and *FET3* mRNA levels (right panel). FOB, ferrioxamine B uptake; FeRed, ferric reductase activity (in copper deficient (-Cu), copper replete (+Cu) or iron deficient (BPS) conditions); Fe(II), ferrous

uptake. Results are expressed (according to the color scale) in log base 2 as the ratio mutant/wild type. Means from 4 experiments.